Status of PRIMA for the VLTI or the quest for user-friendly fringe tracking

C. Schmid[a], R. Abuter[a], S. Ménardi[a], L. Andolfato[a], F. Delplancke[a], F. Derie[a], N. Di Lieto[a], R. Frahm[a], Ph. Gitton[b], N. Gomes[acd], P. Haguenauer[b], S. Lévêque[a], S. Morel[b], A. Müller[ae], T. Phan Duc[a], E. Pozna[a], J. Sahlmann[fa], N. Schuhler[b], G. van Belle[a]

[a]European Southern Observatory (ESO), Karl-Schwarzschild-Strasse 2 , D-85748 Garching, Germany;
[b]ESO, Casilla 19001, Santiago 19, Chile;
[c]SIM - Laboratório de Sistemas, Instrumentação e Modelação em Ciências e Tecnologias do Ambiente e do Espaço, Rua Dr. Roberto Frias, s/n 4200-465 Porto, Portugal;
[d]FCUP - Faculdade de Ciências da Universidade do Porto, Rua do Campo Alegre, s/n, 4169-007 Porto, Portugal;
[e]Max-Planck Institut für Astronomie, Königstuhl 17, D-69117 Heidelberg, Germany;
[f]Observatoire de Genve, Université de Genève, 51 Chemin Des Maillettes, 1290 Sauverny, Switzerland

ABSTRACT

The Phase Referenced Imaging and Micro Arcsecond Astrometry (PRIMA) facility for the Very Large Telescope Interferometer (VLTI), is being installed and tested in the observatory of Paranal. Most of the tests have been concentrated on the characterization of the Fringe Sensor Unit (FSU) and on the automation of the fringe tracking in preparation of dual-field observations. The status of the facility, an analysis of the FSU performance and the first attempts towards dual-field observations will be presented in this paper. In the FSU, the phase information is spatially encoded into four independent combined beams (ABCD) and the group delay comes from their spectral dispersion over 5 spectral channels covering the K-band. During fringe tracking the state machine of the optical path difference controller is driven by the Signal to Noise Ratio (SNR) derived from the 4 ABCD measurements. We will describe the strategy used to define SNR thresholds depending on the star magnitude for automatically detecting and locking the fringes. Further, the SNR as well as the phase delay measurements are affected by differential effects occurring between the four beams. We will shortly discuss the contributions of these effects on the measured phase and SNR noises. We will also assess the sensitivity of the group delay linearity to various instrumental parameters and discuss the corresponding calibration procedures. Finally we will describe how these calibrations and detection thresholds are being automated to make PRIMA as much as possible a user-friendly and efficient facility.

Keywords: Astrometric and interferometric instruments, Interferometry

1. INTRODUCTION

Ground based interferometry suffers from atmospheric turbulence which introduces random Optical Path Difference (OPD) variations causing fringe jitters and wiping out the visibility of interference signals. This leads to strict limitations in the sensitivity of current instruments by imposing short detector integration times in order to freeze the fringe jitter and to recover a useful interference signal.

The PRIMA facility is a system designed to enable simultaneous interferometric observations of two celestial objects - each within a field of 2 arcsec diameter - that are separated by up to 2 arcmin, without requiring a large continuous field of view.[1] It will be able to overcome current sensitivity limitations by using two objects (a

Further author information: (Send correspondence to C.S.)
C.S.: E-mail: cschmid@eso.org, Telephone: +49 (0)89 3200 6467

Optical and Infrared Interferometry II, edited by William C. Danchi, Françoise Delplancke, Jayadev K. Rajagopal,
Proc. of SPIE Vol. 7734, 77340F · © 2010 SPIE · CCC code: 0277-786X/10/$18 · doi: 10.1117/12.857419

bright guide star near a fainter object) to bring some corrections to the atmospheric turbulence. The brighter of the two objects serves to increase the sensitivity on the fainter one: Stabilizing the fringes on the bright object at comparably short detector integration times, and thus correcting for the atmospheric turbulence, allows the observation of the faint object at long exposure times under stable atmospheric conditions with high visibilities.

Depending on the operation mode, PRIMA can be used either to measure the angular separation between the two objects (astrometric mode), or to produce images of the fainter of the two objects using a phase reference technique (imaging mode).

These capabilities will enable the VLTI to address directly a number of extremely important scientific issues that are currently at the top of the list of challenges for future astronomical high resolution instrumentation.

To make this happen PRIMA involves the synergetic interaction of several long-established and newly installed subsystems of the VLTI. The following section gives a short overview on the different new subsystems and summarizes their current status in terms of integration and testing. In the further course of this contribution we will focus on a more detailed analysis of one of the subsystems, namely the FSUs, including considerations about its performance limiting effects and ideas for its user-friendly operation. Finally we will report on first recent attempts towards dual fringe detection.

2. STATUS OF THE FACILITY

PRIMA is composed of four major sub-systems, the Star Separators (STSs), the Differential Delay Lines (DDLs), the PRIma METrology (PRIMET), and the FSUs as well as an overall control system including software. Their current status is summarized in the following.

2.1 Star Separator

In order to simultaneously observe two objects of which the brighter one serves to increase the sensitivity on the fainter one, the signals from the two stars have to be separated, e.g., at the telescope level. The STS is an opto-mechanical system placed at the telescope foci to pick up both objects and to collimate their light separately into two parallel beams. In case of the Auxiliary Telescopes (ATs), to this end, the system includes a derotator, made of three planar mirrors in a motorized rotation stage to compensate for the field rotation, and the STS itself whose central element is a sharp roof mirror to split the telescope field of view in two beams; (a detailed description of the system can be found in Ref. 2). These beams propagate through the interferometer towards the instrument and the two fringe tracker where each pair of beams coming from the same object but from two telescopes forms a fringe pattern. Thereby, the STS supplies also the actuators for the image and pupil stabilization loops.

Two STSs have been delivered to Paranal Observatory, and installed and aligned on AT3 and AT4. Their performance testing was delayed due to lack and failure of some hardware parts and pieces. Meanwhile the STSs are mostly functional and partly commissioned. They have been both equipped with the tip tilt sensors, System for Tip-tilt Removal with Avalanche Photodiodes (STRAP), and holographic notch filters at the Coudé Beam Switching Device (CBSD) to remove stray light of the Delay Line (DL) metrology laser. The only remaining missing part is the Variable Curvature Mirror (VCM) to be used to relay the pupil longitudinally.[3] The hardware will only be delivered at the end of 2011. It is currently replaced by flat or fixed curvature mirrors that relay the pupil correctly for one given baseline that is used during the commissioning periods. Pointing, tracking and field stabilization performance are in line with the AT single-feed performance and with the requirements for PRIMA operation (residual tip-tilt in the laboratory $\approx 0.03''$ rms on sky, lower than the requirement for fringe tracking of $0.1''$ rms). A tip-tilt control using the InfraRed Image Sensor (IRIS) in the laboratory and the STS Field Selector Mirror (FSM) has been implemented and successfully tested at different measurement frequencies up to 100 Hz. Unfortunately, it appeared that the actuator range for the pupil alignment is not large enough to compensate for internal and external pupil misalignment. At the moment, stellar pupils can only be relayed with flat mirrors using settings which are close to the actuator limit. This pupil alignment problem will be fully characterized in terms of the sources of misalignment and corrected during the next commissioning run. During the next mission it is also planned to implement an IRIS guiding mode employing two different Detector

Integration Times (DITs) for the read-out, a short one for the bright primary target and a long one for the dim secondary target.*

2.2 Differential Delay Lines

During PRIMA operation the main DLs compensate the OPD introduced by Earth rotation.[4] However, the angular separation between the two observed objects causes an additional differential OPD which has to be compensated in order to obtain interference fringes on both objects simultaneously. This differential OPD is leveled out for each beam by one DDL.[5] Hence, four DDLs are installed in the interferometric laboratory at Paranal. Each of them uses a cat's eye retro-reflection concept and a two stage actuation system, composed of a motor and a fast linear piezo stage, to introduce the optical delay. To avoid differential dispersion effects affecting the accuracy of the astrometric measurements, each DDL is placed within a vacuum vessel. The DDL position is measured by an internal laser metrology system.

Since August 2008, the four DDLs and related sub-systems have been set-up and aligned in the VLTI laboratory. All four DDLs can be used nominally during PRIMA commissioning runs. In the beginning vacuum vessel 2 suffered from a leak which meanwhile has been partially corrected. The current leak is compliant with the specifications (interval between pumping larger than one week, duration not exceeding 5 hours). Concerning their performance, the DDLs are behaving as expected and as tested in Europe: they exhibit and maintain at the observatory a remarkable dynamic performance (cut-off frequency of $\approx$ 400 Hz $>$ requirement of 200 Hz, high quality, low pure delay). The final DDL metrology alignment system has been installed.

2.3 The Fringe Sensor Units

The two beam pairs coming from the STS and propagating through the VLTI tunnel, the DLs and the DDLs, are combined in the twin fringe sensors of the FSU:[6] FSUA and FSUB. In each of them the two beams originating from the primary or the secondary object, respectively, interfere at a non-polarizing beam splitter cube. In order to retrieve a phase measurement from the interference signal the resulting fringe is sampled at four points with a known separation in phase space. The phase modulation is spatial using polarization multiplexing, i.e., after the beam combination the two beams are further split by polarizing beam splitter cubes to yield four output beams which are coupled into single mode fibers. Using the proper optical components ensures that the four output beams are (ideally) separated by 90° in phase. The outputs of the fibers are imaged on a detector which is placed inside a cryostat. Inside the cryostat the light is spectrally dispersed to allow for group delay estimation. A detailed description of the instrument concept and its implementation can be found in Ref. 6.

Both, FSUA and FSUB are working, can be calibrated and operated. Each of them has been extensively tested in single-feed operation. After initially pushing the limiting magnitude of the system[6] it was concentrated on streamlining the operation, improving the calibration and analyzing the FSU behavior. Schemes have been tested to alleviate the operations burden on the operator, see Sec. 3.2. One of the main factors limiting the FSU performance seems to be the quality of the calibration. The calibration done on the laboratory light source MARCEL is not fully representative of a real operation on sky as the polarization of the various beams is not identical in laboratory and on sky. A calibration scheme on sky could not be tried yet as it requires a full dual-feed operation. It is planned for the coming commissioning runs. As a consequence, a comparably strong non-linearity of the Group Delay (GD) signal and SNR has been identified.[7] Currently, with these restrictions, routine fringe tracking is being achieved with the full PRIMA configuration (including STS and DDL) up to magnitude $m_K = 5$ in standard atmospheric conditions. Improved performance in limiting magnitude (with new algorithm and calibration, with good seeing conditions and finely tuned operation) have still to be established but are expected to be one or two magnitudes higher. Still, a lot of work remains to be done in this respect. Some of the problematic aspects are discussed in more detail in Sec. 3.

2.4 PRIMA Metrology

Before the light captured by the two telescopes interferes at the FSUs it follows a train of 25 mirrors all the way down through the DL tunnel to the interferometric laboratory. Consequently, the fringe signals are affected

*It shall be able to cope with a magnitude difference in K band of $\Delta m_K = 5$.

by static optical path differences and by time-varying optical path fluctuations due to vibrations of mechanical structures, air turbulence inside the interferometer and DL motion. PRIMET is a laser metrology system designed to monitor these instrumental disturbances with an accuracy goal of 5 nm. It is based on two heterodyne Michelson interferometers which are operating simultaneously and which have common paths with the star light inside the VLTI optical train, see Ref. 8 for a more detailed description.

PRIMET has been installed and aligned on both, FSUA and FSUB and can be used for FSU calibration, in conjunction with the laboratory light source MARCEL. One of the two channels, PRIMET-B, has been demonstrated with pupil tracking and fringe stabilization through the DDL and DL out to AT-mounted STS during nighttime conditions. A full test with both channels in real conditions was not yet possible due to the STS pupil alignment problems. However the very first tests (in a non-standard configuration called cyclop mode) are encouraging with a stabilization of the pupil within specifications (< 100 μm jitter) and a very good stability of the metrology signal (no glitches due to the VLTI internal turbulence).

2.5 Software and Control System

The VLTI control system consists of three major parts, the Interferometric Supervisor Software (ISS), the subsystem control software and the instrument software (the latter of which is called PACMAN in the case of PRIMA astrometric mode, see Sec. 2.5.5). For each of these parts, the arrival of PRIMA and all related subsystems at the Paranal Observatory required new installations or diverse modifications, adaptations and extensions of the existing software. Actually, meanwhile the number of lines of code has been doubled in all parts of the software. These necessary changes have been successfully tested in the single- and dual-feed mode.

2.5.1 ISS/PSS

The ISS is the software on the highest hierarchical level of the VLTI Control System. Its main responsibilities are to coordinate the whole VLTI, to configure the array, to support alignment procedures and to provide the external interface. The PRIMA Supervisor Software (PSS) takes care of handling the special PRIMA specific types of presets.

The various modes of the ISS (single-feed with Fringe tracking Instrument NIce TOrino (FINITO) or FSUA/B, Astronomical Multi-BEam combineR (AMBER), Mid-Infrared Interferometric Instrument (MIDI),[9] dual-feed ...) have been extensively tested and the switch from one to the other been made user friendly. Presetting has been tested up to ISS, however, a test at the level of the instrument software PACMAN is still to be done for the dual-feed case. A full preset in dual-feed till four stabilized beams are delivered to the instruments (FSUs) takes usually less than 15 min. The control software is ready for merging with the operational version, i.e. its use is transparent for operations. It has been intensively refined to have an operation as smooth and as similar as possible to the established, classical VLTI operation.

2.5.2 AT-STS Control Software

The function of the Auxiliary Telescope Control Software (ATCS) is to control and operate effectively all the telescope equipment. As the STS in its dedicated Relay Optics Structure (ROS) can be considered as part of the telescope its handling as well as several new functions have to be included in the ATCS for the operation of PRIMA.

A unified version of AT software to handle both configurations of the telescope with/without STS (dual-feed/single-feed ROS) was successfully tested on dual- and single-feed telescopes AT3, AT4 and AT2. The new software version includes in particular the control functions of the STS and the derotator as well as all the different types of PRIMA presets. It is ready for being merged with the current Paranal operational version.

2.5.3 (d)OPDC and DDL software

The Optical Path Difference Controller (OPDC) is responsible for searching, detecting and tracking interferometric fringes. To this end, it uses the signals measured by the fringe sensors (e.g., FINITO or PRIMA FSUs) to compute optical path length corrections in real time and sending these to the tracking DLs. The same holds analogously for the differential Optical Path Difference Controller (dOPDC) and the DDLs; however dOPDC is specific to PRIMA only.

A new software branch of OPDC including the changes needed for PRIMA has been developed and merged with the previous Paranal operational version. The functional parts of the new version related to PRIMA operation have been extensively and successfully tested during single-feed fringe tracking. It was even tested in a non-standard configuration to control the DDLs.

The dOPDC system is installed in Paranal. First tests have been done during the last commissioning period. Tests of its full functionality including DDL blind tracking, fringe detection and fringe tracking on sky in PRIMA dual-feed configuration remain to be done but are envisaged for the near future.

2.5.4 The RMN recorder

The different control systems of the VLTI require to record a large amount of data in real-time, at a high frequency (up to 8 kHz) at many different places (FSU, PRIMET, DDL, IRIS, etc. ...). To this end, they rely on a low latency, deterministic shared memory mechanism, the Reflective Memory Network (RMN) recorder.[10] It communicates in the form of a closed ring, which includes all devices involved in the different control loops. Sensor data, intermediate filtered signals, final actuator set-points and feedbacks flow through this ring, and can be consumed asynchronously by any of its nodes. In fact, those signals are also often the astronomical data itself like, e.g., the beam combiner fluxes for astrometry.

Originally the RMN recorder was developed within the scope of PRIMA but soon turned out to be of general use for other systems of the VLTI. It was adapted and is meanwhile routinely used for engineering purposes. Progress is made in order to offer it soon to reliably record, e.g., FINITO data for AMBER, or other common facility measurements.

2.5.5 PACMAN Instrument Software

PACMAN is the instrument software implemented with the purpose of coordinating the operation of the PRIMA facility at the VLTI with respect to astrometric observations.[11] The PACMAN templates are split in five groups according to the function to be performed:

- A *Calibration* template for the laboratory which is needed to characterize the PRIMA sub-systems on the laboratory light source MARCEL. At the moment its output data is mainly used for diagnostics and health checks of the FSUs. For the future evaluation of astrometric data it will describe the FSU system response consisting of detector dark current as well as the spectral bandpass and relative phases of the optics.
- An *Acquisition* template which does not produce any data file. It is used to point the telescopes including the STSs, to optimize some loops, to set the PRIMA configuration and to finally acquire the four beams fed into the two FSUs.
- A sky *Calibration* template which is basically the same as the laboratory one but performed when the beams are carrying the star light. Thus it characterizes not only the FSU system response but the one of the full VLTI optical train.
- An *Observation* template which produces the data products from which the astrometric narrow angle will be computed.
- Several different *Maintenance* templates have been created to implement requirements that have been deemed necessary from the experiences of the past commissioning periods. They are performed on a regular basis to check that the PRIMA sub-systems are performing as expected and to monitor the stability of their performance.

The laboratory Calibration template has been extensively and successfully tested. The Observation and Acquisition template were successfully used for independent fringe tracking with the FSUs A and B. Their use within the full scope of parallel fringe tracking on sky in dual feed remains to be demonstrated.

3. ANALYSIS OF FSU PERFORMANCE

As already shortly stated in Sec. 2.3 both FSUs have been extensively tested in single-feed operation. Thereby, during the first runs it was tried to investigate the operational limits of the system, while the following commissioning periods were dedicated to streamlining the operation, improving the calibration and analyzing the FSU behavior. The results obtained during the first testing phase are described in detail in Ref. 6. Here, we will concentrate on encountered difficulties during the second testing phase and their possible solutions with regard to operational aspects. In particular we focus on the setting of proper SNR thresholds.

3.1 Differential effects and their impact on the performance

The spatial phase modulation as used in the PRIMA FSU has a number of advantages compared to a temporal scheme. However, a general drawback is that it has to account for differential effects between the four channels, such as differential injection into the single-mode fibers, non-ideal phase separations, differential transmission, effective wavelengths, and pixel response. An accurate calibration is necessary to account for at least some of these instrumental effects.

The calibration parameter space is large and a systematic sensitivity analysis is out of the scope of this contribution. Here, we mention the most important sources of errors.

The current FSU real time algorithm assumes that the fringes recorded in the four channels A, B, C, D have the same wavelength. Contrarily, the calibration run with the laboratory light source MARCEL produces different wavelength estimates for all channels. Although this could be partly due to calibration errors, the main cause is optical distortion of the cold camera, which induces a differential shift of the fiber images formed on the detector, along the dispersion axis of the spectrometer. Hence, the wavelength errors are algorithm and calibration errors. Still the impact is the same, whether they are due to wrong estimation of actual wavelengths or to this limitation of the algorithm.

Phase shift errors are caused by the difference between the phase shifts which are actually present in the VLTI optical train and the ones which are estimated during the calibration procedure and injected in the FSU algorithm. Additionally there is some indication that there is a systematic difference between the phase shifts encountered in the laboratory and the ones faced during on sky observations due to polarization effects of the VLTI optical train.

Errors can also occur on the estimation of the dark and flat fields. As long as they leave the difference of the normalized signal between A and C, or B and D, invariant the FSU algorithm is insensitive to them. Otherwise they result in a cyclic error of the phase delay and the fringe amplitude estimates, with a periodicity of one mean wavelength.

Phase shift and wavelength errors induce cyclic errors of the phase delay and the fringe amplitude with a periodicity of one half mean wavelength. All the cyclic error have a constant amplitude, except those induced by wavelength errors. In the latter case the phase delay error amplitude increases linearly with OPD and the fringe amplitude error increases quadratically.

These cyclic errors make the FSU phase delay and group delay estimates non-linear and the fringe amplitude (used to derive the SNR, see Sec. 3.2) sensitive to OPD jitter. Furthermore, high non-linearities reduce the gain margin of the fringe tracking loops and may cause instability. An analysis of some of the differential effects can be found in Ref. 7.

3.2 SNR – threshold setting and automatic fringe detection

The SNR is one of the three real time estimates of the FSU and serves as the driving input for the OPDC state machine. In case of the FSU the OPDC uses three states according to thresholds which have currently to be specified by the user of the system. The threshold scheme is similar to the one which was originally implemented for FINITO (prior to its extension[12]), see Fig. 1.

The first threshold is the *detection level*. Once the SNR exceeds this level, it indicates the detection of the fringe and the OPDC will try to close the tracking loop.

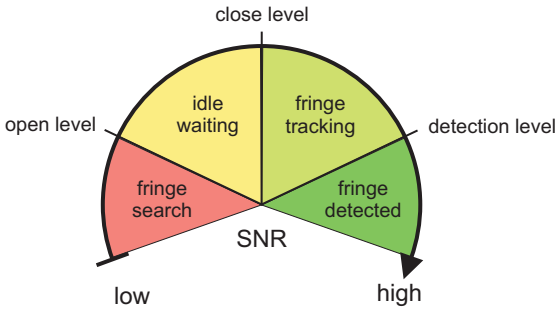

Figure 1. Schematic sketch of the FSU OPDC state machine.

The second threshold is the *close level*. As long as the SNR stays above this level the OPDC will keep the loop closed and try to track the fringes. If the SNR falls below this threshold the OPDC opens the loop but does *not* start a new fringe search. It will keep the delay line position and wait whether the SNR signal recovers. This "idle" behavior is kept until the SNR falls below the third threshold. The main reason for the "idle" state is the fact that a fringe loss can occur not only due to a fringe jump, but also due to flux drops in one of the beams. The latter is caused by bad injection into the FSU single mode fibers due to tip/tilt jitters. It cannot be detected because of lack of photometric channels. Still, the probability for the injection to recover and the fringes to reappear is high, and it might pay off to hold the DL position.

The third threshold is the *open level*. If the SNR falls below this threshold this indicates for the OPDC that the fringes were lost. The OPDC will open the tracking loop and start a new fringe search by scanning with the delay line around the position where the fringes have been lost.

Within this scheme the fringe-tracking control algorithm uses the remaining two real time estimates of the FSU (phase and group delay) to combine both, slow group delay and fast phase tracking. Thereby, the controller tries to keep the group delay signal at zero by tracking at a time varying phase target. The phase estimate is unwrapped if the difference between two consecutive samples is more than π and depends on the integral of the group delay. The integral controller of the group delay uses a time constant of a few seconds which is large compared to the ≈ 0.1 s of the phase controller time constant. This ensures that the control algorithm stays within the central fringe tracking the delay of maximum coherence .

For an un-experienced user the question arises how to set the values for the three thresholds properly. In order to answer this question and possibly even devise an automatic procedure for the setting, it pays off to recall the definition of the FSU SNR, and to have a look which SNR behavior is obtained from the data.

The SNR is defined as the fringe or visibility amplitude of the white light signal inside the fringes $V(t)$, (i.e., at around zero OPD), divided or normalized by the average visibility amplitude of the noise, $\langle v_0(t)\rangle$, (i.e., at an OPD which is large compared to the coherence length of the observed light)[†]:

$$\mathrm{SNR}(t) \equiv \frac{V(t)}{\langle v_0(t)\rangle}. \tag{1}$$

Thereby, the visibility amplitude is given as the norm of the fringe phasor, $V(t) = \sqrt{X_0'^2 + Y_0'^2}$, and the phasor components X_0', Y_0' are derived from the four detector signals of the FSU which are (ideally) in phase quadrature. The visibility amplitude of the noise is estimated on the target during the acquisition of the flat and dark fields within the calibration on sky prior to the fringe tracking.

Given this definition it can be expected that the real time SNR should be distributed around a mean value of 1 as long as the fringes have not been found yet. Indeed this can be confirmed by looking at fringe tracking data obtained between March 2009 and February 2010, see Fig. 2(a). The distribution of the data SNR values is, however, not completely symmetric around 1 which results in a slightly higher mean value of 1.2 with a standard deviation of 0.41.

[†]We follow here the notation and definitions of Ref. 6

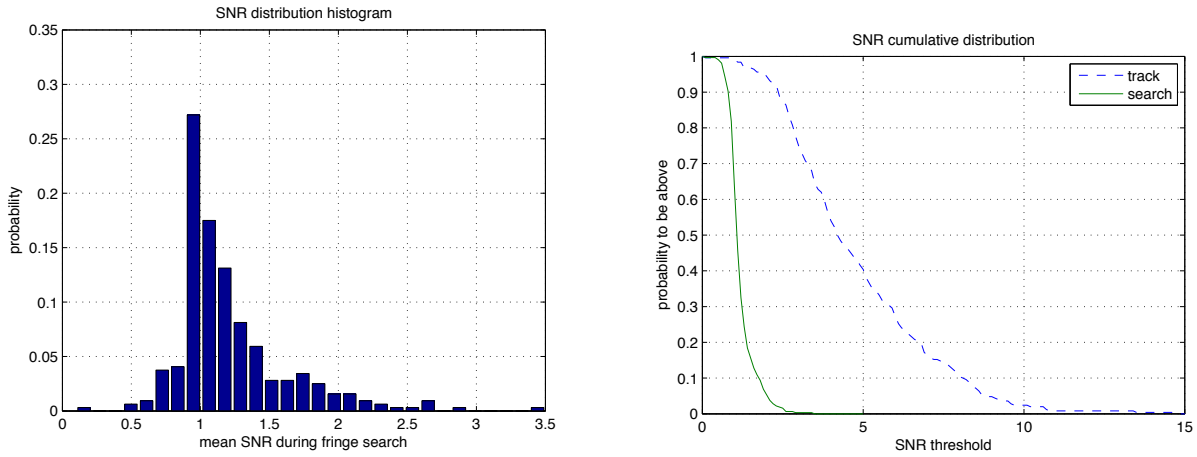

(a) **(b)**

Figure 2. (a) Distribution histogram for the mean value of the SNR during the OPDC state "search", i.e., outside of the fringe (assuming correct setting of the thresholds by the operator). The mean is taken over the time series within each file. The histogram contains fringe tracking files taken between March 2009 and February 2010. (b) Cumulative distribution function of the SNR for OPDC state "search" (–) and "track" (- -). The probability to obtain an SNR value above 2.5 outside of the fringe is only 1.6%

Still, it gives already a first hint on the proper setting of the threshold for the *open level*. Fig. 2(b) displays the cumulative SNR distribution for the taken data in the OPDC state "search" and "track". Assuming that the thresholds have been set correctly by the operator during the recording of this data, these states can be associated with "being outside of the fringe" and "inside the fringe", respectively. As can be seen, noise, i.e., the signal outside of the fringe, should usually not lead to an SNR bigger than 3. For the selected data, the probability to obtain SNR > 2.5 from noise was below $\approx 1.6\%$. This implies that an SNR > 4 can be considered to be caused by a "real" fringe signal; (compare Fig. 2(b) dashed line). In the fringe, the actual SNR value depends on many different parameters such as, e.g., the star's brightness or its intrinsic visibility. As will be seen in the following, the previous considerations do *not* imply that an SNR < 3 cannot be caused by a real fringe signal. In particular for faint stars the SNR inside the fringe can take values between 1.5 and 4. In such instances it might be difficult to distinguish the regimes in which the SNR is caused by real fringes or by noise. Consequently, the proper setting of the thresholds for the *close* and *detection level* is more complicated. Setting the detection level too high can lead to missing the fringes on faint stars. On the other hand, setting it too low can lead to tracking on noise, or for bright stars also to tracking on side lobes.

Fig. 3 shows the mean value of the SNR (with its standard deviation as error bar) depending on the star magnitude in K band, m_K, for OPDC state "track" and "search". While the SNR value outside of the fringe is rather constant across the star magnitude, the SNR signal inside the fringe exhibits a clear dependence. Noticeable is the significant drop for $m_K > 4.5$. The slight decrease in the signal for $m_K < 2$ is due to the reduced intrinsic target visibility for very bright, and hence big and partially resolved, stars. Very similar results on the dependence of the SNR on the star magnitude have been obtained in Ref. 6 for data taken between October 2008 and February 2009.

These observations, in agreement with the experience gained during the operation of the system, suggest that the same, comparatively fixed set of thresholds works for targets with $0 \leq m_K \leq 4.5$. However, it is also clear that the thresholds need to be different in the high magnitude regime.

With respect to decide on the setting of the *detection* and *close level* it is not only helpful to consider the mean value of the SNR inside and outside of the fringe, but another quantity which we call the SNR overlap. It is the overlap between the SNR distribution function inside and outside the fringe, and we choose to mathematically

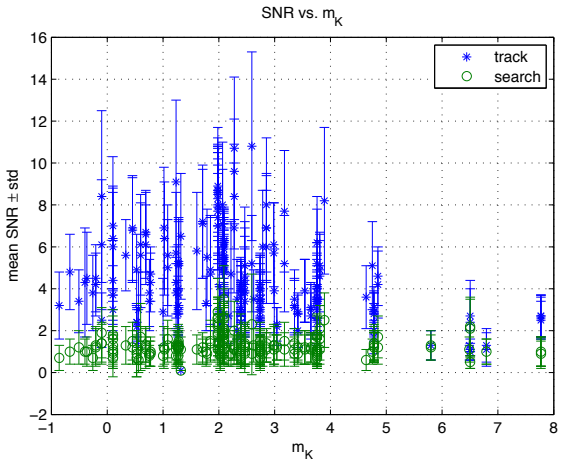

Figure 3. Mean value of the SNR for OPDC state "track" (∗) and "search" (○) versus target magnitude in K band, m_K. The error bars denote the standard deviation. Mean and standard deviation are taken over the time series within each file.

define it as the inner product between two square-integrable functions,

$$\langle f, g\rangle \equiv \int f^*(x)\, g(x)\, \mathrm{d}x, \tag{2}$$

where the functions are normalized such that $\|f\| \equiv \sqrt{\langle f, f\rangle} = 1 = \sqrt{\langle g, g\rangle} \equiv \|g\|$. This ensures that the overlap is a quantity reaching from 0, "no overlap", to 1, "maximal overlap"[‡]. As the analytical form of the distribution functions of the SNR inside and outside of the fringe is not known, it is numerically sampled at n points for each data file, such that Eqn. 2 reads

$$\langle \vec{s}^{\,\mathrm{in}}, \vec{s}^{\,\mathrm{out}}\rangle = \sum_{i=1}^{n} s_i^{\mathrm{in}} s_i^{\mathrm{out}}. \tag{3}$$

Fig. 4 shows a typical example for data recorded in June 2009 on the star HD167314, ($m_K = 2.4$). Already in the time series of the SNR, Fig. 4(a), it is clearly visible when fringes are present. In agreement with what was stated before, the SNR outside of the fringe is distributed approximately around 1.1 ± 0.7, see Fig. 4(b), compare Fig. 2(a). The SNR inside the fringe is with 4.2 ± 1.2 a bit low but still in agreement with the observations made in the context of Fig. 3. Fig. 4(c) displays the according cumulative distribution functions. Clearly visible in Fig. 4(b) is the overlapping region in which the SNR signal is ambiguous; there it might be caused either by real fringes or pure noise. Using Eqn. 3 the overlap can be quantified to be 0.06.

In general, the overlap increases for fainter targets. As a consequence also the cumulative distribution function inside the fringe will approach the one outside the fringe for faint objects. It is obvious that the higher the overlap is, the more difficult it is to keep fringe tracking due to the afore mentioned ambiguity. From Fig. 4(c) it can be seen that when setting in the example the detection threshold to 3 there is only a probability of 1.2% for the noise to trigger a fringe detection. At the same time, 15% of the real fringe signal will not be detected, which is still passable. However, for an increasing overlap the latter percentage will increase, and it is impossible to lower it without increasing the probability to trigger fringe detections by noise when lowering the threshold value.

The observations made on the evaluated data so far imply the following suitable strategy to set the SNR thresholds:

The *detection level* should be set around the mean of the distribution function inside the fringe (or even slightly higher). This ensures that the fringe detection is, to a very high probability, caused by real fringes. The *close level* should be set right in the middle of the overlapping region. In case that the signal drops to this level

[‡]An overlap value of 1 means rather that no fringes are visible at all.

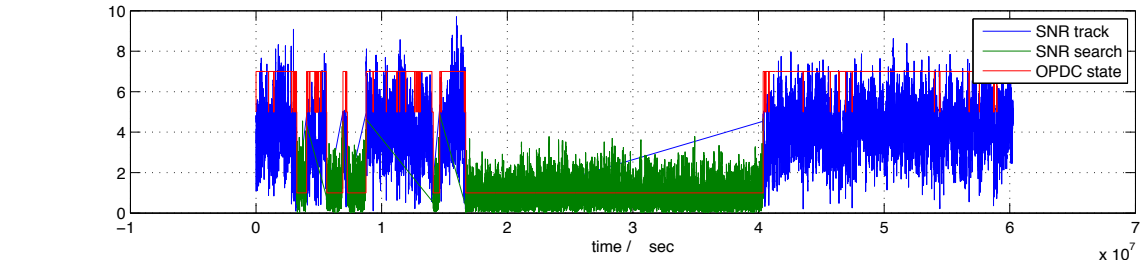

(a)

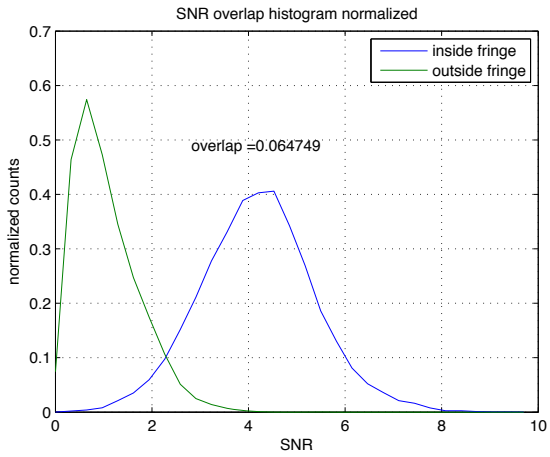

(b)

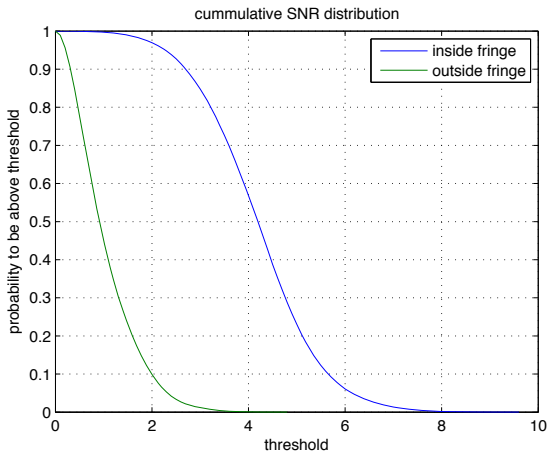

(c)

Figure 4. (a) Time series of the SNR and the OPDC state (–) observed on the target HD167314, ($m_K = 2.4$). OPDC state 7 corresponds to "track", 5 to "idle", 1 to "search" (compare Fig. 1). (b) SNR distribution function outside (–) and inside (–) the fringe. The overlap between the two functions is 0.06. (c) Cumulative distribution function of the SNR outside (–) and inside (–) the fringe.

one cannot be sure anymore whether it comes from fringes or from noise. Then it seems sensible to open the loop and wait how the signal evolves. If it rises again the fringes are still there and tracking can be restarted. If it decreases even further it indicates that the fringes are lost and a new search might be necessary. Therefore, the *open level* should be set around the mean of the SNR distribution function outside of the fringe.

For the example in Fig. 4(b) the proper thresholds would be hence approximately 4.2/2.5/1, for *detection/close/open*, and these were indeed the values used for the recording of this file. During the mission in June 2009 this set of thresholds worked well over the whole range of targets up to $m_K = 4.5$. Only slight modifications around these values were necessary from time to time[§]. In practice it is reasonable to start with these values. Once the fringes are found, a file can be recorded and the values be iteratively refined by evaluating the data off line. For fainter stars no suitable set of thresholds has been tried yet. However, in case that the operator is not certain about the threshold setting we propose to scan the fringes using the DLs. This was successfully done in February 2010. Fig. 5 shows the result for the star CD-47 8012B ($m_K = 6.2$). Usually in such a scan the fringe can be easily identified and the SNR values derived by applying the strategy discussed above.

4. FIRST ATTEMPTS TOWARDS DUAL-FIELD OBSERVATIONS

In February 2010, for the first time, the STSs installed on AT3 and AT4 were in a condition which allowed in principle parallel fringe detection with both FSUs.

[§]In particular in the case of a very noisy signal the *open level* could be set a bit higher, e.g., to 1.2, in order to avoid that the fringes are completely lost before restarting the search again.

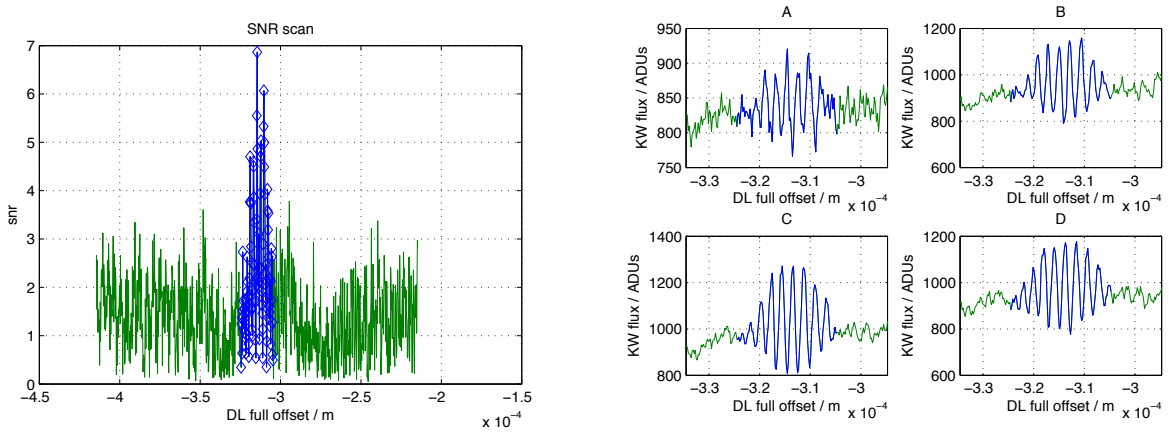

(a) (b)

Figure 5. Scan across the fringes using the DL for the star CD-47 8012B ($m_K = 6.2$) recorded on FSUA. The scan range was 200 µm; the scanning time was 10 s. (a) SNR signal versus DL full offset: (–) denotes noise and (-◇-) the fringe. (b) Detector signals during the scan for the four channels A, B, C, D. (–) denotes noise and (–) the fringe.

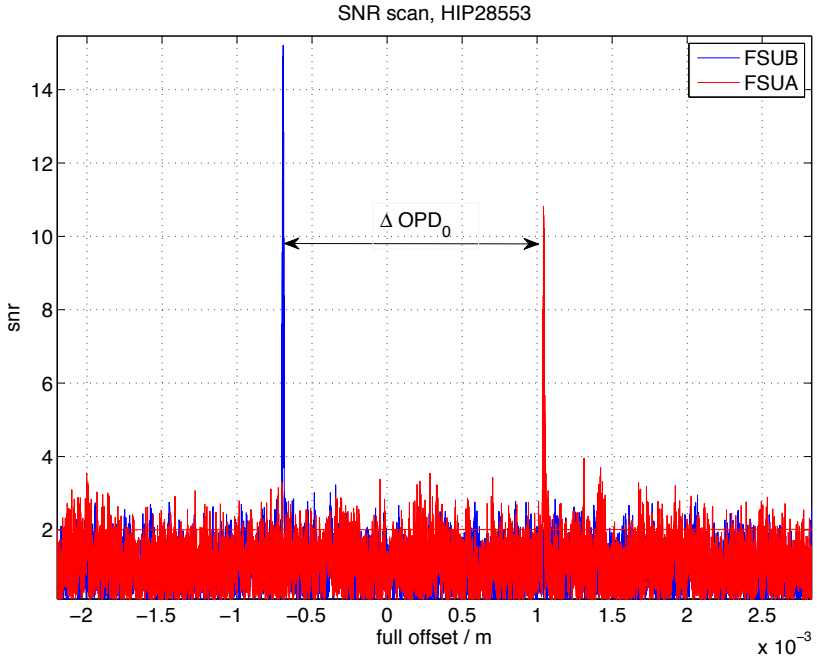

Figure 6. SNR signal during a fringe scan for the star, HIP28553 ($m_K = 3.7$), recorded with FSUA (–) and FSUB (–), *sequentially*. The star was swapped from the A to the B feed using the STS derotator.

In preparation for the dual feed fringe detection, fringes were consecutively searched and detected on a single star, HIP28553 ($m_K = 3.7$) with FSUB *and* FSUA. The target was swapped from the B to the A feed by using the derotator. The detection of the fringes for the same star with different FSUs allows to estimate ΔOPD_0, which is the OPD difference between the A and B feed arising from manufacturing and positioning errors of the mirrors within the dual feed optical train. Fig. 6 shows the obtained result in terms of a SNR scan, from which ΔOPD_0 can be determined to be approximately 1.7 mm. The OPD model used for these scans was still premature. Its uncertainty on the baseline length led to a fringe drift at a speed of about 35 $\frac{\text{nm}}{\text{s}}$. Taking this into account together with the time difference between the two fringe detections, the uncertainty on the value of ΔOPD_0 is estimated to be about ±66 µm. Although this result was obtained from a single measurement only

and needs to be corroborated in the future, it is sufficient to conclude that the OPD difference between the two feeds is on a order of magnitude that can be easily compensated by the DDLs.

It can be also seen from Fig. 6 that the performance of FSUA is worse than the one of FSUB with respect to the SNR signal. The maximal SNR for FSUA is with 10.8 only two third of the one of FSUB which is 15.2. The reason for this is still under investigation.

Due to lack of time the simultaneous fringe detection on both FSUs for a dual star was not successfully accomplished. However, we are confident that this will be achieved during the next mission.

5. SUMMARY AND OUTLOOK

In this contribution we gave a short overview on the current status of PRIMA and its subsystems. We focused in particular on one subsystem, the FSU, outlining some identified problems and advising a strategy to facilitate the operation of the system.

In general, the effort during the PRIMA commissioning periods held so far was concentrated on each subsystem individually. Some of the subsystems have been operated together, but a functional verification of PRIMA as a whole, means as instrument, involving the interaction between all relevant instances is still outstanding. Nevertheless, we are determined to approach this goal in the near future. The stage for it is set with regard to most of the subsystems. Although the functionality is mostly covered, it is also clear from the previous considerations that some work remains to be done for improvements concerning understanding, performance and operability of the subsystems. These are, however, enduring efforts to be done in parallel to the functional tests and to be finished on a longer time scale. In the further course of 2010 two missions in Paranal are already scheduled which will mark the transition from test activities on subsystem- to full system-level. They shall comprise the test of the DDL blind trajectory and the parallel operation of PRIMET with the FSUs to finally achieve dual-feed observations of pairs of stars with fringe detections in FSUA and FSUB simultaneously.

ACKNOWLEDGMENTS

We acknowledge various support by staff of the Paranal Observatory, in particular to mention the assistance by the Telescope Instrument Operators (TIOs). C.S. and R.A. thank J.-B. Le Bouquin for stimulating discussions.

REFERENCES

[1] F. Derie, F. Delplancke, A. Glindemann, S. Lévêque, S. Ménardi, F. Paresce, R. Wilhelm, and K. Wirenstrand, "PRIMA technical description and implementation," in *Proceedings of GENIE - DARWIN Workshop - Hunting for Planets (ESA SP-522)*, H. Lacoste, ed., June 2002.

[2] F. Delplancke, J. Nijenhuis, H. de Man, L. Andolfato, R. Treichel, J. Hopman, and F. Derie, "Star separator system for the dual-field capability (PRIMA) of the vlti," in *Society of Photo-Optical Instrumentation Engineers (SPIE) Conference Series*, W. A. Traub, ed., *Presented at the Society of Photo-Optical Instrumentation Engineers (SPIE) Conference* **5491**, pp. 1528–+, Oct. 2004.

[3] M. Ferrari, G. R. Lemaitre, S. P. Mazzanti, F. Derie, A. Huxley, J. Lemerrer, P. Lanzoni, P. Dargent, and A. Wallander, "Variable curvature mirrors: implementation in the vlti delay-lines for field compensation," *Interferometry for Optical Astronomy II* **4838**(1), pp. 1155–1162, SPIE, 2003.

[4] F. Derie, "Vlti delay lines: design, development, and performance requirements," *Interferometry in Optical Astronomy* **4006**(1), pp. 25–30, SPIE, 2000.

[5] F. Pepe, D. Queloz, T. Henning, A. Quirrenbach, F. Delplancke, L. Andolfato, H. Baumeister, P. Bizenberger, H. Bleuler, B. Chazelas, F. Derie, L. D. Lieto, T. P. Duc, O. Duvanel, M. Fleury, D. Gillet, U. Graser, F. Koch, R. Launhardt, C. Maire, D. Megevand, Y. Michellod, J.-M. Moresmau, P. Mullhaupt, V. Naranjo, L. Sache, Y. Salvade, G. Simond, D. Sosnowska, K. Wagner, and L. Zago, "The espri project: differential delay lines for prima," *Optical and Infrared Interferometry* **7013**(1), p. 70130P, SPIE, 2008.

[6] J. Sahlmann, S. Ménardi, R. Abuter, M. Accardo, S. Mottini, and F. Delplancke, "The prima fringe sensor unit," *A&A* **507**, pp. 1739–1757, Dec. 2009.

[7] J. Sahlmann, R. Abuter, S. Menardi, C. Schmid, N. D. Lieto, F. Delplancke, R. Frahm, P. Gitton, N. Gomes, P. Haguenauer, S. Leveque, S. Morel, A. Mueller, T. P. Duc, N. Schuhler, and G. van Belle, "First results from fringe tracking with the prima fringe sensor unit," in *These proceedings*, 2010.

[8] S. A. Leveque, R. Wilhelm, Y. Salvade, O. Scherler, and R. Daendliker, "Toward nanometer accuracy laser metrology for phase-referenced interferometry with the vlti," *Interferometry for Optical Astronomy II* **4838**(1), pp. 983–994, SPIE, 2003.

[9] A. Müller, J.-U. Pott, S. Morel, R. Abuter, G. van Belle, R. van Boekel, L. Burtscher, F. Delplancke, T. Henning, W. Jaffe, C. Leinert, B. Lopez, A. Matter, K. Meisenheimer, C. Schmid, K. Tristram, and A. Verhoeff, "First results using prima fsu as a fringe tracker for midi," in *These proceedings*, 2010.

[10] R. Abuter, D. Popovic, E. Pozna, J. Sahlmann, and F. Eisenhauer, "The vlti real-time reflective memory data streaming and recording system," *Optical and Infrared Interferometry* **7013**(1), p. 70134A, SPIE, 2008.

[11] R. Abuter, "Pacman: the prima astrometric instrument software," in *These proceedings*, 2010.

[12] J.-B. L. Bouquin, R. Abuter, B. Bauvir, H. Bonnet, P. Haguenauer, N. di Lieto, S. Menardi, S. Morel, F. Rantakyrö, M. Schoeller, A. Wallander, and S. Wehner, "Fringe tracking at vlti: status report," *Optical and Infrared Interferometry* **7013**(1), p. 701318, SPIE, 2008.